Title

A single microRNA miR-195 rescues the arrested B cell development induced by EBF1 deficiency

Authors

Y. Miyatake[1], T. Kamakura[2], T. Ikawa[3], R. Yanagiya[1], R. Kotaki[1], K. Kameda[1], R. Koyama-Nasu[4,5], K. Okuyama[6], K. Hirano[7], H. Hosokawa[7], K. Hozumi[7], M. Ohtsuka[8], T. Kishikawa[9], C. Shibata[9], M. Otsuka[10], R. Maruyama[11], K. Ando[12], T. Kurosaki[13,14,15], H. Kawamoto[16], and A. Kotani[1,2*]

Affiliations

[1] Department of Innovative Medical Science, Tokai University School of Medicine, Isehara, Kanagawa, 259-1193, Japan

[2] Department of Regulation of Infectious Cancer, Research Institute for Microbial Diseases, The University of Osaka, Suita, 565-0871, Osaka

[3] Division of Immunology and Allergy, Research Institute for Biomedical Sciences, Tokyo University of Science, Noda, Chiba, 278-0022, Japan

[4] Department of Immunology, Graduate School of Medicine, Chiba University, Chiba, Chiba, 260-0856, Japan

[5] Department of Experimental Immunology, Graduate School of Medicine, Chiba University, Chiba, Chiba, 260-0856, Japan

[6] Laboratory for Transcriptional Regulation, RIKEN Center for Integrative Medical Sciences, Yokohama, Kanagawa, 230-0045, Japan

24 [7] Department of Immunology, Tokai University School of Medicine, Isehara,
25 Kanagawa, 259-1193, Japan

26 [8] Department of Molecular Life Science, Tokai University School of Medicine,
27 Isehara, Kanagawa, 259-1193, Japan

28 [9] Department of Gastroenterology, Graduate School of Medicine, The University of
29 Tokyo, Bunkyo-ku, Tokyo, 113-0033, Japan

30 [10] Department of Gastroenterology and Hepatology, Okayama University Hospital,
31 Okayama, Okayama, 700-8558, Japan

32 [11] Project for Cancer Epigenomics, Cancer Institute, Japanese Foundation for Cancer
33 Research, Koto-ku, Tokyo, 135-8550, Japan

34 [12] Hematology and Oncology, Research Institute for Radiation Biology and Medicine,
35 Hiroshima University, Hiroshima, Hiroshima, 734-8551, Japan

36 [13] Laboratory of Lymphocyte Differentiation, WPI Immunology Frontier Research
37 Center, Osaka University, Suita, Osaka, 565-0871, Japan

38 [14] Laboratory for Infectious Disease Education and Research, Osaka University, Suita,
39 Osaka, 565-0871, Japan

40 [15] Laboratory for Lymphocyte Differentiation, RIKEN Center for Integrative Medical
41 Sciences, Yokohama, Kanagawa, 230-0045, Japan

42 [16] Laboratory of Immunology, Institute for Life and Medical Sciences, Kyoto
43 University, Kyoto, Kyoto, 606-8507, Japan

44 *Corresponding author. Email: aikotani@k-lab.jp

45

Abstract

Accumulated studies have reported that hematopoietic differentiation was primarily regulated by transcription factors. Early B cell factor 1 (EBF1) is an essential transcription factor for B lymphopoiesis. Contrary to the canonical notion, we found that a single miRNA, miRNA-195 (miR-195) transduction let EBF1 deficient hematopoietic progenitor cells (HPCs) express CD19, carry out V(D)J recombination and class switch recombination, which implied that B cell matured without EBF1. A part of the mechanism was caused by FOXO1 accumulation via inhibition of FOXO1 phosphorylation pathways in which targets of miR-195 are enriched. These results suggested that some miRNA transductions could function as alternatives to transcription factors.

Introduction

Developmental hierarchy in hematopoiesis has been widely researched, and it is well-known that proper stimulation leads hematopoietic stem cells (HPCs) into B cell lineage. Lineage specification is primarily regulated at the transcriptional level, thus lineage-specific transcription factors are considered to indispensable for differentiation (*1*, *2*). B cell development requires multiple transcription factors, especially Early B cell Factor 1 (EBF1), Paired Box 5 (Pax5), and E2A. Pax5 and E2A are critical transcription factors for early B cell development, but they cannot rescue EBF1-deficient HPCs from failure of B cell lineage commitment (*3*). Conversely, ectopic expression of EBF1 is able to rescue Pax5, E2A, and PU.1 deleted progenitor cells from B lymphopoiesis arrest, and thus EBF1 is considered more potent than the other transcription factors (*2*, *4*, *5*). As the

69 most potent transcription factor, EBF1 is essential for pre-pro-B cell to become pro-B
70 cell; namely, *Ebf1*$^{-/-}$ cell express B220 but is disable to express CD19 (*6*).

71 MicroRNAs (miRNAs) are small non-coding RNA containing approximately 22
72 nucleotides that regulate several target protein expressions mediating deadenylation and
73 translation by post-transcriptionally repressing or decaying target messenger RNAs
74 (mRNAs) (*7–10*). Although similar to transcription factor, miRNAs regulate large
75 numbers of target mRNAs and deeply contribute to various cell events, the regulation is
76 mainly required for negative regulation of leaky gene expression and often called as
77 fine-tuning (*11*, *12*). In hematopoiesis, miRNAs are expressed in lineage specific
78 manner and their profiles greatly influence on cell differentiation (*13–15*). Focusing on
79 B cell development, it is revealed that Dicer, a key enzyme of miRNA generation, is
80 essential for pre- to pro- B cell transition (*16*). Individual miRNA is also studied and
81 miR-150 and miR-126 are identified as relational factor to B cell lineage development.
82 miR-150 regulate B cell differentiation by controlling c-Myb expression and miR-126
83 partially rescues EBF1 deficient B cell lineage commitment by modulating IRS-1
84 expression (*17*, *18*). Both miRNAs dramatically contributed to B cell development
85 processes, but they were not able to recover B cell development from EBF1 deficiency.
86 Conceived from these vigorous functions of miRNAs on B cell development, in this
87 time, we analyzed ability of miR-195, recently revealed as an important factor for
88 several cell differentiation, on B cell lineage commitment in EBF1 deficient HPCs (*19*,
89 *20*).
90

91 **Results**

92 **miR-195 induces B cell character in EBF1 deficient HPCs**

93 To assess the contribution of miR-195 on B cell development, miR-195 was transduced
94 into mouse fetal liver (FL)-derived Lin$^-$ c-kit$^+$ HPCs and the cells were differentiated to
95 B220 and CD19 expressing pro-B cells with IL7, Flt ligand and SCF on OP9 stroma cells.
96 After 7 days of culture, certain numbers of the cells gradually expressed CD19, and the
97 positive cells was increased by miR-195 transduction (Fig. 1A). This result suggests that
98 miR-195 has ability to shift the HPCs differentiation toward B cells. Next, we attempted
99 to differentiate *Ebf1*$^{-/-}$ FL HPC to B cell with miR-195 transduction (Fig. 1B). As by a
100 previous study (*6*), control *Ebf1*$^{-/-}$ FL HPCs expressed B220 but did not express CD19.
101 However, miR-195 transduced *Ebf1*$^{-/-}$ FL HPCs highly expressed CD19 (Fig. 1C). In
102 normal B cell development, CD19 expression follows B220 expression and hence CD19
103 positive cells show B220 expression as well. Thus, miR-195-transduced *Ebf1*$^{-/-}$ FL HPCs
104 which including B220 negative CD19 positive population may simply reflect up-
105 regulation of CD19 expression, but not B cell development. To exclude this possibility,
106 gene expressions of miR-195-transduced *Ebf1*$^{-/-}$ FL HPCs by cDNA microarray assay
107 were investigated then indicated that miR-195-transduced cells more expressed B cell
108 lineage related genes, e.g., *Pax5, Aicda*, *Rag1*, *Rag2*, *CD79b* and *Runx2*, whereas less
109 expressed T cell and NK cell lineage related genes, including *Gata3, Id2*, *Lck*, *CD3e* and
110 *Il2rb* and also myeloid lineage related genes for example, *Cebpe*, *Ly6g*, *Fcgr1*, *Fcgr2b*
111 and *fcgr3* (Fig. 1D). (1-6) Among the B-lineage transcription factors, *Pax5* and *Erg* were
112 modestly but significantly upregulated ($\log_2$FC ~1.2 and ~0.9, respectively) in miR-195-
113 transduced *Ebf1*$^{-/-}$ cells compared to controls. While these changes were moderate, they
114 were consistent across replicates and suggest partial restoration of the B cell
115 transcriptional program. These results suggested that not only CD19 expression but also

116 up-regulation of several B cell developmental factors and down-regulation of other
117 lineage related genes were involved in the promotion of B cell lineage commitment by
118 miR-195.
119
120 **EBF1 deficient HPCs were able to commit B cell lineage by transduction of miR-195**
121 **with bone marrow niche modification**
122 The ectopic miR-195 expression led *Ebf1*$^{-/-}$ HPCs induced differentiation toward B cell.
123 However, a large part of the miR-195-transduced HPCs expressed CD19 but not B220,
124 which implied that they strayed from the canonical B cell differentiation steps (Fig. 1C).
125 In addition to the inner state, the microenvironment known as niche was also critically
126 involved in hematopoiesis (*21*). Especially in early B cell development, bone marrow
127 niches precisely control the maintenance and differentiation of lineage precursors by
128 cytokines and chemokines (*22*). To explore the development of miR-195-transduced
129 *Ebf1*$^{-/-}$ FL HPCs under bone marrow niches, we engrafted miR-195-transduced *Ebf1*$^{-/-}$
130 early B cells into NOG and B6RG mice, in which absence of B cell makes the engrafted
131 B cell visible (Fig. 2A). After 7 days, the engrafted cells successfully adapted in the bone
132 marrow. While there was no remarkable change in control cell population, notably,
133 instead of B220 negative CD19 positive cells, the double positive cells were markedly
134 increased in miR-195-transduced *Ebf1*$^{-/-}$ FL early B cells, suggesting that the normal
135 stepwise B cell development occurred (Fig. 2B). In B cell development, most prominent
136 steps after CD19 expression are VDJ recombination and subsequential IgM expression
137 on cell surface. In addition to CD19 expression, EBF1 is also known as essential gene for
138 VDJ recombination, especially V_H to DJ_H recombination (*23*). To determine whether
139 miR-195-transduced *Ebf1*$^{-/-}$ cells rearranged the VDJ region, we attempt to detect V_H-J_H

140 assembled gene segments in the engrafted mouse bone marrow cells by droplet digital
141 PCR (ddPCR). The data revealed that there were certain number of V_H-J_H segments in
142 the bone marrow of mice engrafted miR-195-transduced *Ebf1*$^{-/-}$ cells (Fig. 2C, Fig. S1).
143 Subsequently, to expect the EBF1 independent reconstitution enabled B cell receptor to
144 express as IgM, we analyzed B cell populations in the engrafted mouse bone marrow. Not
145 much but some miR-195-transduced cells expressed IgM on cell surface likely as normal
146 immature B cell in bone marrow 10 days after engraftment (Fig. 2D). Moreover, these
147 IgM positive cells were also detected in splenocytes. These data suggested that engrafted
148 cells had differentiated into IgM positive immature or mature B cells, and they have been
149 recruited to spleen. The critical function of B cell is changing B cell receptor from IgM
150 to IgG following class switch DNA recombination, which is accompanied by stimuli-
151 induced cell proliferation. To clarify whether miR-195-transduced *Ebf1*$^{-/-}$ B cells have the
152 function, whole splenocyte of the engrafted mice were stimulated with IL-4 and LPS,
153 which causes class switch recombination to IgG1 (*24*). While control transduced GFP
154 positive cells did not expand by the stimuli, miR-195-transduced GFP positive cells
155 expanded enough to be surely detected and importantly a part of them expressed IgG1
156 (Fig. 2E). These data suggested that miR-195 has a potential to induce B cell
157 differentiation from HPCs to mature B cells, resulting in class switch recombination even
158 when critical regulator EBF1 is absent.
159

160 **miR-195 physiologically maintains several B cell populations**

161 As ectopic miR-195 expression revealed its potential in B cell development. Next, to
162 investigate contribution of endogenous miR-195 for B cell lineage populations, miR-195
163 deficient mice in which the genome around miR-195-5p was eliminated by CRISPR/Cas9

164 system were established. The analysis of HPC lineage populations in the bone marrow
165 revealed that several B cell-related progenitors were relatively reduced in miR-195$^{-/-}$ mice.
166 Sca-1^{-} c-kit^{+} common myeloid progenitor cell population was increased but
167 controversially, Sca-1^{+} c-kit^{-} (LSK^{-}) cells was decreased in miR-195$^{-/-}$ mice (Fig. 3A). As
168 LSK^{-} cells mainly includes early lymphoid precursor, these results suggested that miR-
169 195 is involved in hematopoiesis including differentiation of stem cells toward lymphoid
170 and early B cells (*25*). While analysis of each early B cell populations did not show
171 significant difference, whole B220^{+} IgM^{-} pre B cell populations was slightly increased in
172 the BM of miR-195$^{-/-}$ mice (Fig. 3B). In the splenic B cells, marginal zone B (MZB) cells
173 were reduced in miR-195$^{-/-}$ mice (Fig. 3C). MZB cells was previously reported to be
174 highly dependent on EBF1 activity and disappear in absence of EBF1. B-1 cells was
175 likewise crucially regulated EBF1 as well(*26*). In the peritoneal cavity of miR-195$^{-/-}$ mice,
176 B-1 cells were significantly decreased (Fig. 3D). These results suggested that miR-195
177 contributed to maintain several EBF1-dependent mature B cell populations at least in a
178 part. Taken together, these results were consistent with those obtained from ectopic
179 expression of miR-195.
180

181 **FOXO1 phosphorylation pathway targeted by miR-195 was responsible for B cell**
182 **lineage commitment**

183 To elucidate how miR-195 promote B cell development in EBF1 deficient HPCs, we
184 analyzed regulatory networks of predicted miR-195 target genes by using starBase_v2.0
185 and David Bioinformatics Resources 6.8 in KEGG pathway database (*27–33*). Several
186 gene regulation networks were detected as candidates of responsible pathways on the
187 miR-195 function (Table S1 and S2). Remarkably, MAPK signaling pathway and PI3K-

188 Akt signaling pathway included various targets of miR-195. Both MAPK and Akt were
189 known to phosphorylate and degradate FOXO1, which was a critical factor in several
190 stages of B cell development (*34*). Thereby, we focused on the predicted miR-195 targets:
191 *Pik3r1*, *Pdpk1*, *Akt3*, *Raf1*, *Sos2,* and *Mapk3*, which were involved in and activate MAPK
192 and PI3K-Akt pathways. First, to confirm that the predicted targets are actually regulated
193 by miR-195, we picked up 3'UTR of *Mapk3* and *Akt3,* which were especially important
194 in the pathways, and inserted in a luciferase reporter assay plasmid. As expected, the
195 luciferase activity was down-regulated by miR-195 transduction, but it was not impaired
196 by transduction of miR-195 mutant of mature miRNA region (Fig. 4A). Furthermore, to
197 determine whether the predicted targets were actually regulated by miR-195, we
198 measured the expression levels in miR-195-transduced *Ebf1*$^{-/-}$ HPCs, and qPCR analysis
199 showed that miR-195 transduction certainly decreased the mRNA levels (Fig. 4B).
200 Because of sequence similarity among miR-15/16 family members, the baseline levels
201 detected in control samples may include signal from endogenous miRNAs such as miR-
202 497 or miR-16. Thus, the observed increase ($\log_2$FC ~2.5) may underestimate the actual
203 level of miR-195 overexpression. In line with these findings, *Mapk3* expression was also
204 downregulated in our microarray analysis of miR-195-transduced *Ebf1*$^{-/-}$ cells. However,
205 for *Akt3*, the microarray results were inconsistent across different probes, suggesting
206 probe-dependent variability. Therefore, while qPCR and reporter assays support *Akt3* as
207 a potential target of miR-195, its regulation remains to be further validated. Next, to
208 evaluate inhibition of FOXO1 phosphorylation and degradation by miR-195, we
209 compared protein levels of FOXO1 and phosphorylated FOXO1 (pFOXO1) in miR-195-
210 transduced *Ebf1*$^{-/-}$ HPCs. The western blotting results revealed that miR-195 transduction
211 decreased pFOXO1 levels and increased relative FOXO1 protein levels (Fig. 4C, Fig. S2).

212 We also performed western blotting for PAX5 and ERG using the same samples. The
213 results showed no significant change in these protein levels between miR-195-transduced
214 and control Ebf1$^{-/-}$ cells (Fig. S3), consistent with the modest upregulation observed in
215 our microarray data. Finally, to determine whether FOXO1 accumulation is sufficient for
216 *Ebf1*$^{-/-}$ HPCs to differentiate into pro-B cells, *Ebf1*$^{-/-}$ HPCs were transduced with *Foxo1*
217 and cultured under the B cell differentiating condition. Similar to miR-195 transduction,
218 Foxo1 transduction arose B220 and CD19 double positive *Ebf1*$^{-/-}$ cells, which was
219 accompanied with CD19 positive but B220 negative population (Fig. 4D). These data
220 indicated that FOXO1 accumulation by inhibition of phosphorylating pathways was
221 responsible for *Ebf1*$^{-/-}$ HPCs to differentiate into B cell lineage.
222
223 **Epigenetically activated genes in pro-B cells by miR-195 is fewer than by EBF1**
224 In B cell development, epigenetic changes of transcription factors and differentiation
225 molecules are crucial for proper development, which are mainly regulated by EBF1 (*35*,
226 *36*). We investigated transposase-accessible chromatin using deposited sequencing data
227 (ATAC-seq) of *Ebf1*$^{-/-}$ pro-B cells and wild type pro-B cells from GSE92434 and cells in
228 early B cell lineages from GSE100738. While wild type pro-B cells/ *Ebf1*$^{-/-}$ pro-B cells
229 differentially accessible (DA) ATAC peaks were observed in 2809 sites, wild type CD19
230 positive/ CD19 negative early B cells DA ATAC peaks were in 904 sites. Then, 678 sites
231 were overlapped, which were considered to be regulated by EBF1 as important locus for
232 early B cell development. Moreover, some of them were overlapped with miR-195-
233 transduced B220 and CD19 double positive *Ebf1*$^{-/-}$ cells (miR-195 CD19+) / B220
234 positive CD19 negative *Ebf1*$^{-/-}$ cells (control CD19-) DA ATAC peaks (73 out of 226
235 peaks), which were considered to be regulated by miR-195 (Fig. 5B). These peaks

236 included important genes for early B cell development, such as *Pax5*, *Runx1*, *Erg*, *Ifr8*,
237 and *Blnk*, and B cell-related genes, such as *Rarres1*, *Ciita*, and *Atg7* (Table S3). These
238 results indicated that gene locus opened by miR-195 were fewer than by EBF1, but they
239 included several key locus for B cell differentiation, and they were enough to differentiate
240 the progenitor cells to mature B cells. Moreover, HOMER Motif Analysis revealed that
241 enriched motives opened by EBF1 and by miR-195 were 198 and 111, respectively (Fig.
242 5C). The common motives were 104 which included critical genes for B cell development,
243 such as E2A, Foxo1, and PAX5, and high ranked motives were very similar between
244 EBF1 and miR-195 (Fig. 5D). These results suggested that miR-195 transduction opened
245 important chromatin regions for early B cells, which were normally regulated by EBF1.
246 Finally, we concluded that miR-195 transduction was able to compensate EBF1
247 deficiency in B cell development through activation of FOXO1 and epigenetic regulation
248 of several B cell-related genes.
249
250
251 **Discussion**
252 The canonical notion of hematopoietic fate determination implies that EBF1 is an
253 indispensable factor for B lymphopoiesis. However, in this study, we showed that a single
254 microRNA miR-195 rescued the arrest of pro-B cell differentiation induced by EBF1
255 deficiency. As miRNA plays roles in a bundle of their family, single miRNA deficient
256 mice often do not show significant phenotype (*37*). Nevertheless, miR-195 deficient mice
257 showed not much but sure decreased number of several hematopoietic cells including
258 marginal zone B cells and peritoneal B-1 cells, which were reported to almost disappear
259 in EBF1^{ihCd2} mice in which EBF1 was deficient in mature B cells (*38*). Considering that

260 other miRNA deficient mice have subtle phenotype and miR-195 is one of the large
261 family, including miR-15/16 and miR-195/497 (*39*), the remarkable potential of miR-
262 195 is beyond a fine tuner as microRNA, at least as far as it is considered with regard to
263 B cell lineage commitment.

264 A part of the mechanisms of the potent function of miR-195 was caused by inhibition of
265 phosphorylation of FOXO1. FOXO1 is a transcriptional factor controlled by EBF1 and
266 strongly promote differentiation of pre-B cell. FOXO1 activity is regulated by
267 PI3K/AKT pathway and several miRNAs were reported to be involved in the regulation
268 (*40*). We showed *Foxo1* transduction enable EBF1 deficient cell to express CD19.
269 However, the CD19 positive cells rapidly disappeared and couldn't be detected in
270 transplanted mice (data not shown). It is presumable that FOXO1 activity was necessary
271 to express CD19, but other factors undertake maintenance and proliferation of the
272 developing cells. ATAC-seq analysis revealed that miR-195 was directly or indirectly
273 involved in chromatin accessibility. As the chromatin regions and motives opened by
274 miR-195 were critical for B cell differentiation and hematopoiesis, further investigation
275 is needed for the mechanism.

276 Although our study indicates that miR-195 has the potential to promote B cell lineage
277 commitment in the absence of EBF1, the precise downstream targets and mechanisms
278 remain only partially defined. We hypothesize that the observed effects are mediated
279 through the downregulation of multiple mRNA targets involved in opposing B-lineage
280 differentiation, including kinases in the MAPK and PI3K-Akt pathways that modulate
281 FOXO1 phosphorylation. While our microarray, qPCR, and luciferase assays support
282 the regulation of specific targets such as *Mapk3* and *Akt3*, a more comprehensive

283 identification of direct targets—especially those related to transcriptional and epigenetic
284 regulation—would further strengthen our conclusions. We interpret our findings as
285 revealing the potential of miR-195 to compensate for EBF1 deficiency, rather than a
286 demonstration of its physiological role. Future studies using global transcriptome,
287 proteome, and chromatin-binding assays will be essential to fully elucidate the
288 mechanisms underlying this observation.

289 To compensate for the lack of transcriptome data from sorted *miR-195*-transduced pre-
290 pro-B or CD19+ *Ebf1*$^{-/-}$ cells, we compared our microarray data with publicly available
291 RNA-seq profiles of *Ebf1*$^{-/-}$ pro-B cells (GSE92434). This analysis revealed that several
292 B-lineage defining genes downregulated in *Ebf1* deficiency were upregulated upon
293 miR-195 expression, suggesting that miR-195 may partially restore transcriptional
294 programs disrupted by the loss of EBF1.

295 Although direct evidence of FOXO1 binding to B-lineage gene loci (e.g., via ChIP-seq
296 or CUT&RUN) is currently lacking due to technical limitations in cell numbers, our
297 results suggest that FOXO1 plays a key functional role. This is supported by its
298 increased protein level upon miR-195 expression, the partial phenocopy by FOXO1
299 overexpression, and the enrichment of FOXO1 motifs in open chromatin regions
300 identified by ATAC-seq. Future studies incorporating FOXO1 chromatin profiling will
301 be important to validate its direct regulatory role in this context.

302 While ddPCR provided a sensitive means to detect *VH-JH* rearranged fragments, it does
303 not offer resolution of specific V, D, or J gene usage or recombination completeness.
304 Therefore, the full extent and diversity of V(D)J recombination in *Ebf1*$^{-/-}$ miR-195-

305 induced CD19^{+} cells remains to be clarified. Future studies incorporating high-
306 throughput sequencing approaches will be important to fully characterize the
307 immunoglobulin repertoire and confirm progression through the pre-BCR checkpoint.

308 While our data support the B-lineage identity of miR-195-induced *Ebf1*$^{-/-}$ CD19^{+} cells
309 based on gene expression, chromatin accessibility, and immunoglobulin expression, we
310 have not directly tested their lineage plasticity under alternative differentiation
311 conditions. Whether these cells retain responsiveness to myeloid cytokines or exhibit
312 residual multipotency remains to be determined. Future studies using single-cell fate
313 mapping or in vitro differentiation assays will be required to fully define the lineage
314 commitment status of this population.

315 While our results demonstrate that ectopic expression of miR-195 can compensate for
316 the loss of EBF1 in promoting B cell development, we acknowledge that this does not
317 necessarily reflect a physiological role for miR-195. The miR-195 knockout mice
318 exhibited only mild alterations in B cell populations, suggesting that under normal
319 conditions, miR-195 is not essential for B lymphopoiesis. Therefore, our findings
320 should be interpreted as highlighting the potential of miR-195 to modulate B cell fate
321 under specific conditions, rather than indicating its requirement in physiological B cell
322 development. Further studies will be needed to determine whether miR-195 plays a
323 more prominent role under stress or disease contexts, or in cooperation with other
324 miRNAs.

325 The luciferase activity was markedly reduced in the presence of the Akt3 3'UTR, even
326 in cells transduced with a control vector (Fig. 4A). We hypothesize that the Akt3 3'UTR

327 contains strong post-transcriptional regulatory elements—such as AU-rich elements or
328 binding sites for endogenous miRNAs or RNA-binding proteins—which may suppress
329 mRNA stability or translation independent of miR-195. Alternatively, the secondary
330 structure or length of the UTR may inherently reduce luciferase expression.

331

332 **Materials and Methods**

333 **Plasmid construction**

334 To construct MDH1-PGK-GFP-miR-195, genomic DNA was first extracted from
335 RS4;11 using the DNeasy Tissue Extraction Kit (Qiagen). Next, a segment around miR-
336 195 was amplified by means of PCR, using Pfx polymerase (Invitrogen) and the
337 oligonucleotides, 5′ -AGATCTCTCGAGAAGGAGAGGGTGGGGTAT-3′ and 5′ -
338 GGGGCGGAATTCGCTATTCCCGCATAAGCA-3′. The obtained PCR product was
339 then cloned into the XhoI-EcoRI site of MDH1-PGK-GFP 2.0 (Addgene #11375). To
340 construct pMYs-RFP-Foxo1, first, pEX-Foxo1 (in which mouse Foxo1 is optimized for
341 gene synthesis; Eurofins Genomics K.K.) was synthesized and inserted into the EcoRI-
342 XhoI site of pEX. Next, the Foxo1 region was extracted using the restriction enzymes
343 and inserted into pMYs-RFP retroviral vector (kindly provided by Prof. T. Kitamura,
344 Tokyo University). For in vitro transcription of small-guide RNA (sgRNA), pUC57-
345 195sg-upstream and -downstream were generated. Both plasmids originated from the
346 pUC57-sgRNA expression vector (Addgene #51132), and the annealed oligonucleotides
347 were inserted into a BsaI site (For the former, 5′ -
348 TAGGCCCACAAAGGCAGGGACCTA-3′ and 5′ -
349 AAACTAGGTCCCTGCCTTTGTGGG-3′ were annealed, while for the latter, 5′ -

350 TAGGGGAAGTGAGTCTGCCAATAT-3′ and 5′ -
351 AAACATATTGGCAGACTCACTTCC-3′ were annealed). For the Dual-Luciferase®
352 assay, psiCHECK-2 vector was purchased from Promega and the 3′ -UTRs of Akt3 and
353 Mapk3 were inserted between the XhoI and NotI sites. MDH1-PGK-GFP-miR-195-mut
354 was generated by mutating 6 bases, from the second to seventh bases of the mature
355 miR-195 and complimentary regions of the stem loop structure in MDH1-PGK-GFP-
356 miR-195. In detail, normal miR-195 stem loop sequence 5′ -
357 AGCUUCCCUGGCUCUAGCAGCACAGAAAUAUUGGCACAGGGAAGCGAGUC
358 UGCCAAUAUUGGCUGUGCUGCUCCAGGCAGGGUGGUG-3′ (mature miR-195-
359 5p sequence 5′ -UAGCAGCACAGAAAUAUUGGC-3′) was mutated to 5′ -
360 AGCUUCCCUGGCUCUgcgccgACAGAAAUAUUGGCACAGGGAAGCGAGUCU
361 GCCAAUAUUGGCUGUcggcgcCCAGGCAGGGUGGUG-3′ (mature sequence 5′ -
362 UgcgccgACAGAAAUAUUGGC-3′).
363 **Animals**
364 C57BL/6 mice were purchased from CLEA Japan Inc. NOD/Shi-scid, IL-2RγKO
365 (NOG) and B6RG mice were purchased from Central Institute for Experimental
366 Animals (CIEA). The Ebf1$^{-/+}$ mice were originally generated by R. Grosschedl (*41*).
367 miR-195-deficient mice were generated based on the CRISPR/Cas9 system established
368 by C. Gurumurthy (*42*), using pUC57-195sg-upstream and -downstream for sgRNA
369 expression and pBGK (Addgene #65796) for Cas9 mRNA expression. Sanger
370 sequencing confirmed a deletion of 5,103 base pairs at chromosome 11
371 (GRCm38/mm10 chr11:70,234,425–70,235,103), encompassing the entire *miR-497*
372 sequence upstream and 61 bp of the 93-bp *miR-195* precursor. The deletion was
373 validated using genomic DNA and aligned to the mouse reference genome. All

374 transgenic mice used for experiments were backcrossed to the C57BL/6 background for
375 at least eight generations to minimize off-target effects. The obtained mice were
376 subsequently bred and housed at Tokai University. All the animal experiments in this
377 study complied with the Guidelines for the Care and Use of Animals for Scientific
378 Purposes at Tokai University. To reduce the number of sacrificed animals, the sample
379 sizes for each animal experiment were empirically determined from previous studies or
380 the results of the first littermate mice.

381 **Flow cytometry analysis**

382 Cells were collected and washed in FACS buffer (phosphate-buffered saline
383 supplemented with 2% fetal bovine serum) and subsequently stained with the following
384 antibodies purchased from BioLegend : anti-c-kit (2B8), -Sca-1 (D7), -IL7Rα (A7R34),
385 -B220 (RA3-6B2), -IgM (RMM-1), -CD3ε (145-2C11), -CD4 (GK1.5), -CD8 (53-6.7),
386 -CD11b (M1/70), -CD19 (1D3), -CD23 (B3B4), and -IgG1 (RMG1-1) and Thermo
387 Fisher : anti-Flt3 (A2F10), -CD43 (eBioR2/60), and -CD21/35 (eBio8D9). All samples
388 were analyzed on the BD FACSVerse™ system and the data obtained was analyzed
389 using FlowJo. FACSAria™ III was used for cell sorting.

390 **Culture of lineage-negative (Lin^{-}) cells from the fetal liver**

391 Fetal livers were harvested from pregnant C57BL/6 or *Ebf1*$^{+/-}$ mice (mated with
392 *Ebf1*$^{+/-}$ male) at 13.5 days after vaginal plug formation and minced gently by means of
393 pipetting. The cell suspensions were filtered through a 67-µm pore nylon mesh and Lin^{-}
394 cells were collected using the Lineage Cell Depletion Kit, mouse and AutoMACS® Pro
395 Separator (Miltenyi Biotec), according to the manufacturer's instructions. Subsequently,
396 the collected Lin^{-} cells were transduced with miR-195 or *Foxo1* by means of retroviral
397 transfection. In brief, Platinum-E cells were transfected with MDH1-PGK-GFP (for

398 EMPTY sample) or MDH1-PGK-GFP-miR-195 or pMYs-RFP-Foxo1 using PEI
399 MAX® (Polysciences Inc.), and retroviral supernatants were harvested 48 hours later.
400 Lin$^-$ cells were infected with the supernatants using 10 µg/mL Polybrene (Sigma-
401 Aldrich). The infected and transduced Lin$^-$ cells were cultured and differentiated into B
402 cells on OP9 cells in IMDM (Thermo Fisher) supplemented with 10% fetal bovine
403 serum, 1 mM sodium pyruvate, 0.1 mM non-essential amino acid solution, 50 µM 2-
404 mercaptoethanol, 100 units/mL penicillin G, 100 µg/mL streptomycin (all from Wako),
405 and 10 ng/mL recombinant SCF, IL-7, and Flt3-ligand (R&D Systems). Cells were
406 cultured on OP9 cells for 7 days before analysis unless otherwise specified. For *in vivo*
407 analysis of B cell development of EBF1$^{-/-}$ Lin$^-$ cells, 1×10^6 cells were injected into the
408 NOG or B6RG mice after >7 days of culture and expansion *in vitro*.

409 **Microarray analysis**

410 Total RNA was isolated using the RNeasy MINI Kit (Qiagen), and its quality was
411 analyzed using the 2100 Bioanalyzer (Agilent Technologies). Approximately 100 ng
412 RNA was labeled, and gene expression microarray analysis was performed using the
413 Agilent Whole Mouse Genome Microarray 4x44K v2 (Agilent Technologies),
414 according to the manufacturer's instructions. The processed data was analyzed using
415 GeneSpring GX version 14.9 (Agilent Technologies). Raw intensity values were
416 normalized using the 75th percentile and transformed to the Log_2 scale. All experiments
417 were carried out in duplicates.

418 **Droplet digital PCR (ddPCR)**

419 To carry out ddPCR for VJ recombination analysis, total DNA was isolated from whole
420 cells of the bone marrow in miR-195-transduced *Ebf1*$^{-/-}$ FL HPCs-engrafted NOG mice,
421 using the Wizard® Genomic DNA Purification Kit (Promega). ddPCR was conducted

422 using QX100 Droplet Digital PCR system (Bio-Rad). Briefly, 3.3 μL of template cDNA
423 with 20× primer and a TaqMan™ probe set was partitioned into approximately 20,000
424 droplets using the QX100 Droplet Generator, for amplification. The cycling conditions
425 were 95°C for 10 min, followed by 50 cycles of 95°C for 15 sec and 60°C for 1 min,
426 and a final 10-min incubation at 98°C. The droplets were subsequently read
427 automatically using the QX10 droplet reader. The data were analyzed with QuantaSoft
428 analysis software (ver. 1.3.2.0; Bio-Rad). The primers used were as follows: forward
429 primer – 5′-GAGGACTCTGCRGTCTATTWCTGTGC-3′; reverse primer – 5′-
430 CCCTGACCCAGACCCATGT-3′; and probe – 5′-6FAM-
431 TTCAACCCCTTTGTCCCAAAGTT-TAM-3′.

432 **Class-switch stimulation**

433 EBF1$^{-/-}$ Lin^{-} cells were transduced with EMPTY and miR-195-expressing vector and
434 transplanted into B6RG mice. At 10 days post-transplantation, the spleens were
435 collected from the mice, minced with slide glasses, and filtered through a 67-μm pore
436 nylon mesh. IgM^{+} cells were sorted and stimulated for 3 days with 12.5 μg/mL
437 lipopolysaccharide (Sigma-Aldrich) and 7.5 ng/mL IL-4 (Peprotech) in RPMI-1640
438 (Wako) supplemented with 10% fetal bovine serum, 100 U/mL penicillin G, and 100
439 μg/mL streptomycin.

440 **Gene Ontology analysis**

441 The miR-195 targetomes were gathered from the miR-195 target mRNAs identified
442 from three databases (Targetscan, miRDB, and microRNA.org) and by comparing the
443 microarray data of the targets in control- and miR-195-transduced Ebf1$^{-/-}$ FL HPCs. To
444 investigate the biological functions, these genes were applied to the Gene Ontology
445 classification using GeneSpringGX11.

446 **Quantitative real-time PCR**

447 For mRNA quantification, total RNA was isolated using Sepasol-RNA I Super G
448 (Nacalai Tesque) and cDNA was synthesized from it using the ReverTra Ace™ qPCR
449 RT Master Mix (TOYOBO). qPCR was performed using THUNDERBIRD™ SYBR®
450 qPCR Mix (TOYOBO) on the StepOnePlus™ Real-Time PCR System (Thermo
451 Fisher). The following primers were used for qPCR: Pik3r1 – 5′-
452 AAACTCCGAGACACTGCTGA-3′ and 5′-GAGTGTAATCGCCGTGCATT-3′;
453 Pdpk1 – 5′-CTGGGCTCTGCTCTAGTGTT-3′ and 5′-
454 CCCAGGTTCAGGACAGGATT-3′; Akt3 – 5′-
455 GTGGACCACTGTTATAGAGAGAACAT-3′ and 5′-
456 TTGGATAGCTTCCGTCCACT-3′; Raf1 – 5′-TCTTCCATCGAGCTGCTTCA-3′ and
457 5′-GGATGTAGTCAGCGTGCAAG-3′; Sos2 – 5′-AACTTTGAAGAACGGGTGGC-3′
458 and 5′-TTTCCTGCAGTGCCTCAAAC-3′; and Mapk3 – 5′-
459 ACTACCTGGACCAGCTCAAC-3′ and 5′-TAGGAAAGAGCTTGGCCCAA-3′. For
460 miR-195 quantification, TaqMan™ MicroRNA Assay (ABI) was used. Briefly, total
461 RNA was isolated using Sepasol-RNA I Super G and cDNA was synthesized from it
462 using the microRNA TaqMan™ MicroRNA Reverse Transcription Kit (Thermo Fisher)
463 and a specific primer, 5′-UAGCAGCACAGAAAUAUUGGC-3′. The expression levels
464 were measured using the TaqMan™ Fast Advanced Master Mix (Thermo Fisher) on the
465 StepOnePlus™ Real-Time PCR System. Given the high sequence similarity among
466 miR-15/16 family members, the TaqMan assay for miR-195 may detect related
467 miRNAs such as miR-16. Therefore, we interpreted miR-195 qPCR results as
468 approximate estimates rather than precise quantification. GAPDH was used for
469 normalization to maintain consistency with other qPCR assays in this study. All

470 reagents and kits in this section were used according to the manufacturer's instructions.
471 Target RNA expression levels were compared with those of GAPDH using the $2^{-\Delta\Delta Ct}$
472 method.

473 **Dual-Luciferase® assay**

474 293T cells were co-transfected with 20 ng psiCHECK-2 of *Akt3* or *Mapk3* and 100 ng
475 MDH1-PGK-GFP-miR-195 or MDH1-PGK-GFP-miR-195-mut. At 48 hrs post-
476 transfection, the relative amounts of Renilla and firefly luciferase were analyzed using a
477 Dual-Luciferase® Reporter Assay System (Promega). The Renilla/firefly luciferase ratio
478 was calculated and normalized against the control.

479 **Western blot**

480 Total proteins were collected from whole cells using radioimmunoprecipitation assay
481 buffer (Wako) with protease inhibitor cocktail (Sigma-Aldrich) and SDS sample buffer
482 (60 mM Tris-HCl pH 6.8, 2% SDS, 10% glycerol, and 50 mM dithiothreitol). The
483 proteins were separated using SDS-PAGE and the western blot signal was detected and
484 analyzed using the Immobilon Western Chemiluminescent HRP Substrate (Millipore)
485 on Ez-Capture MG AE-9300 (ATTO). The following antibodies were used: anti-
486 FOXO1 (C29H4, Cell Signaling Technology), -phospho-FOXO1(Ser256) (9461, Cell
487 Signaling Technology), and -GAPDH (G9545, Sigma-Aldrich). Signal intensities were
488 quantified using ImageJ version 1.54g (*43*).

489 **ATAC-seq analysis**

490 For ATAC-seq analysis, $B220^+$ $CD19^+$ and $B220^+$ cells were sorted from the bone
491 marrow of NOG mice transplanted with miR-195-transduced $EBF1^{-/-}$ Lin^- cells. $B220^+$
492 cells were also sorted from the empty transduced sample. The collected cells were
493 resolved using CELLBANKER® (Takara Bio) and temporarily preserved at –20°C.

494 ATAC-seq libraries were prepared from the cryopreserved cells according to the Omni-
495 ATAC protocol (*44*). Briefly, >5,000 cells were lysed and subjected to a transposition
496 reaction. The transposed fragments were pre-amplified, quantitated using RT-PCR, and
497 then amplified again. The prepared libraries were sequenced on the NextSeq 550
498 platform (Illumina) with paired-end reads (read 1, 75 bp; index 1, 8 bp; index 2, 8 bp;
499 read 2, 75 bp). Short-read data were trimmed using sickle 1.33
500 (https://github.com/najoshi/sickle) and mapped onto a mm10 reference genome using
501 bowtie2. Unmapped, multi, chrM mapping, and duplicate reads were eliminated using
502 samtools 1.16.1 and Picard Tools (Picard MarkDuplicates;
503 http://broadinstitute.github.io/picard). Peak summits in all populations were determined
504 using the MACS3 functions (-callpeak -p 1e-5 https://github.com/macs3-
505 project/MACS). Motif enrichment analysis was carried out using HOMER, with default
506 settings.

507 **Statistical analysis**

508 One-sample *t*-test was used to analyze differences between groups, and *p*-values<0.05
509 were considered statistically significant. All analyses were performed using Excel
510 (Microsoft). Statistical significance was determined using the Fisher's exact test,
511 followed by multiple test corrections using the Benjamini and Yekutieli false discovery
512 rate method.

513

514 **Acknowledgments**

515 We thank N. Kurosaki, K. Takahashi, E. Nagashima, and members of the Department of
516 Innovative Medical Science at Tokai University for their assistance, advice, and helpful

517 discussions. We also thank the Support Center for Medical Research and Education at
518 Tokai University for their technical assistance.

519 **Funding:**

520 This work was supported by Grants-in-Aid for Scientific Research JP20H03716 (to A.K.)
521 and JP20K17362 (to Y.M.) from the Japan Society for the Promotion of Science; P-
522 PROMOTE 22ama221213 and 22ama221215 (to A.K.) from the Japan Agency for
523 Medical Research and Development; and JST-CREST JPMJCR19H5 (to A.K.) from the
524 Japan Science and Technology Agency.

525 **Author contributions:**

526 A.K. designed the research; Y.M., T.K., R.Y., R.K., K.K., R.-K.N., and K.O. performed
527 the research; T.I., K. Hirano, H.H., K. Hozumi, M. Ohtsuka, T. Kishikawa, C.S., M.
528 Otsuka, R.M., K.A., and T. Kurosaki contributed new reagents and analytic tools; H.K.
529 analyzed the data; Y.M., T.K., and A.K. wrote the paper.

530 **Competing interests:**

531 The authors declare that they have no conflict of interest.

532 **Data and materials availability:**

533 The microarray data was deposited in Gene Expression Omnibus with the identifier
534 GSE246669, and the ATAC-seq data was also deposited with the identifier GSE246530.
535 The other data generated in this study are available in the manuscript or supplementary
536 materials.

537

538 **References**

539 1. J. Zhu, S. G. Emerson, Hematopoietic cytokines, transcription factors and lineage
540 commitment. *Oncogene* **21**, 3295–3313 (2002).

541 2. T. Ikawa, H. Kawamoto, L. Y. T. Wright, C. Murre, Long-Term Cultured E2A-
542 Deficient Hematopoietic Progenitor Cells Are Pluripotent. *Immunity* **20**, 349–360
543 (2004).

544 3. Y. C. Lin, S. Jhunjhunwala, C. Benner, S. Heinz, E. Welinder, R. Mansson, M.
545 Sigvardsson, J. Hagman, C. A. Espinoza, J. Dutkowski, T. Ideker, C. K. Glass, C.
546 Murre, A global network of transcription factors, involving E2A, EBF1 and
547 Foxo1, that orchestrates B cell fate. *Nature Immunology* **11**, 635–643 (2010).

548 4. J. M. R. Pongubala, D. L. Northrup, D. W. Lancki, K. L. Medina, T. Treiber, E.
549 Bertolino, M. Thomas, R. Grosschedl, D. Allman, H. Singh, Transcription factor
550 EBF restricts alternative lineage options and promotes B cell fate commitment
551 independently of Pax5. *Nature Immunology* **9**, 203–215 (2008).

552 5. I. Györy, S. Boller, R. Nechanitzky, E. Mandel, S. Pott, E. Liu, R. Grosschedl,
553 Transcription factor Ebf1 regulates differentiation stage-specific signaling,
554 proliferation, and survival of B cells. *Genes Dev.* **26**, 668–682 (2012).

555 6. K. L. Medina, J. M. R. Pongubala, K. L. Reddy, D. W. Lancki, R. DeKoter, M.
556 Kieslinger, R. Grosschedl, H. Singh, Assembling a Gene Regulatory Network for
557 Specification of the B Cell Fate. *Developmental Cell* **7**, 607–617 (2004).

558 7. D. P. Bartel, MicroRNAs: Target Recognition and Regulatory Functions. *Cell* **136**,
559 215–233 (2009).

560 8. R. W. Carthew, E. J. Sontheimer, Origins and Mechanisms of miRNAs and
561 siRNAs. *Cell* **136**, 642–655 (2009).

562 9. D. Cifuentes, H. Xue, D. W. Taylor, H. Patnode, Y. Mishima, S. Cheloufi, E. Ma,
563 S. Mane, G. J. Hannon, N. D. Lawson, S. A. Wolfe, A. J. Giraldez, A Novel
564 miRNA Processing Pathway Independent of Dicer Requires Argonaute2 Catalytic
565 Activity. *Science* **328**, 1694–1698 (2010).

566 10. N. Yamakawa, K. Okuyama, J. Ogata, A. Kanai, A. Helwak, M. Takamatsu, K.
567 Imadome, K. Takakura, B. Chanda, N. Kurosaki, H. Yamamoto, K. Ando, H.
568 Matsui, T. Inaba, A. Kotani, Novel functional small RNAs are selectively loaded
569 onto mammalian Ago1. *Nucleic Acids Res* **42**, 5289–5301 (2014).

570 11. C. Sevignani, G. A. Calin, L. D. Siracusa, C. M. Croce, Mammalian microRNAs: a
571 small world for fine-tuning gene expression. *Mamm Genome* **17**, 189–202 (2006).

572 12. M. Listowski, E. Heger, D. Bogusławska, B. Machnicka, K. Kuliczkowski, J.
573 Leluk, A. Sikorski, microRNAs: fine tuning of erythropoiesis. *Cellular and*
574 *Molecular Biology Letters* **18**, 34–46 (2013).

575 13. S. Monticelli, K. M. Ansel, C. Xiao, N. D. Socci, A. M. Krichevsky, T.-H. Thai,
576 N. Rajewsky, D. S. Marks, C. Sander, K. Rajewsky, A. Rao, K. S. Kosik,
577 MicroRNA profiling of the murine hematopoietic system. *Genome Biology* **6**, R71
578 (2005).

579 14. J. R. Neilson, G. X. Y. Zheng, C. B. Burge, P. A. Sharp, Dynamic regulation of
580 miRNA expression in ordered stages of cellular development. *Genes Dev.* **21**, 578–
581 589 (2007).

582 15. C.-Z. Chen, L. Li, H. F. Lodish, D. P. Bartel, MicroRNAs Modulate
583 Hematopoietic Lineage Differentiation. *Science* **303**, 83–86 (2004).

584 16. S. B. Koralov, S. A. Muljo, G. R. Galler, A. Krek, T. Chakraborty, C.
585 Kanellopoulou, K. Jensen, B. S. Cobb, M. Merkenschlager, N. Rajewsky, K.
586 Rajewsky, Dicer Ablation Affects Antibody Diversity and Cell Survival in the B
587 Lymphocyte Lineage. *Cell* **132**, 860–874 (2008).

588 17. C. Xiao, D. P. Calado, G. Galler, T.-H. Thai, H. C. Patterson, J. Wang, N.
589 Rajewsky, T. P. Bender, K. Rajewsky, MiR-150 Controls B Cell Differentiation by
590 Targeting the Transcription Factor c-Myb. *Cell* **131**, 146–159 (2007).

591 18. K. Okuyama, T. Ikawa, B. Gentner, K. Hozumi, R. Harnprasopwat, J. Lu, R.
592 Yamashita, D. Ha, T. Toyoshima, B. Chanda, T. Kawamata, K. Yokoyama, S.
593 Wang, K. Ando, H. F. Lodish, A. Tojo, H. Kawamoto, A. Kotani, MicroRNA-
594 126–mediated control of cell fate in B-cell myeloid progenitors as a potential
595 alternative to transcriptional factors. *PNAS* **110**, 13410–13415 (2013).

596 19. H. Qiu, J. Zhong, L. Luo, Z. Tang, N. Liu, K. Kang, L. Li, D. Gou, Regulatory
597 Axis of miR-195/497 and HMGA1-Id3 Governs Muscle Cell Proliferation and
598 Differentiation. *International Journal of Biological Sciences* **13**, 157–166 (2017).

599 20. A. Dueñas, A. Expósito, M. del M. Muñoz, M. J. de Manuel, A. Cámara-Morales,
600 F. Serrano-Osorio, C. García-Padilla, F. Hernández-Torres, J. N. Domínguez, A.
601 Aránega, D. Franco, MiR-195 enhances cardiomyogenic differentiation of the
602 proepicardium/septum transversum by Smurf1 and Foxp1 modulation. *Sci Rep* **10**,
603 9334 (2020).

604 21. A. C. Gomes, T. Hara, V. Y. Lim, D. Herndler-Brandstetter, E. Nevius, T.
605 Sugiyama, S. Tani-ichi, S. Schlenner, E. Richie, H.-R. Rodewald, R. A. Flavell, T.
606 Nagasawa, K. Ikuta, J. P. Pereira, Hematopoietic Stem Cell Niches Produce
607 Lineage-Instructive Signals to Control Multipotent Progenitor Differentiation.
608 *Immunity* **45**, 1219–1231 (2016).

609 22. K. Tokoyoda, T. Egawa, T. Sugiyama, B.-I. Choi, T. Nagasawa, Cellular Niches
610 Controlling B Lymphocyte Behavior within Bone Marrow during Development.
611 *Immunity* **20**, 707–718 (2004).

612 23. J. M. R. Pongubala, D. L. Northrup, D. W. Lancki, K. L. Medina, T. Treiber, E.
613 Bertolino, M. Thomas, R. Grosschedl, D. Allman, H. Singh, Transcription factor
614 EBF restricts alternative lineage options and promotes B cell fate commitment
615 independently of Pax5. *Nat Immunol* **9**, 203–215 (2008).

616 24. M. Muramatsu, V. S. Sankaranand, S. Anant, M. Sugai, K. Kinoshita, N. O.
617 Davidson, T. Honjo, Specific Expression of Activation-induced Cytidine
618 Deaminase (AID), a Novel Member of the RNA-editing Deaminase Family in
619 Germinal Center B Cells*. *Journal of Biological Chemistry* **274**, 18470–18476
620 (1999).

621 25. R. Kumar, V. Fossati, M. Israel, H.-W. Snoeck, Lin−Sca1+Kit− Bone Marrow
622 Cells Contain Early Lymphoid-Committed Precursors That Are Distinct from
623 Common Lymphoid Progenitors. *The Journal of Immunology* **181**, 7507–7513
624 (2008).

625 26. B. Vilagos, M. Hoffmann, A. Souabni, Q. Sun, B. Werner, J. Medvedovic, I. Bilic,
626 M. Minnich, E. Axelsson, M. Jaritz, M. Busslinger, Essential role of EBF1 in the
627 generation and function of distinct mature B cell types. *Journal of Experimental*
628 *Medicine* **209**, 775–792 (2012).

629 27. J.-H. Yang, J.-H. Li, P. Shao, H. Zhou, Y.-Q. Chen, L.-H. Qu, starBase: a database
630 for exploring microRNA–mRNA interaction maps from Argonaute CLIP-Seq and
631 Degradome-Seq data. *Nucleic Acids Res* **39**, D202–D209 (2011).

632 28. J.-H. Li, S. Liu, H. Zhou, L.-H. Qu, J.-H. Yang, starBase v2.0: decoding miRNA-
633 ceRNA, miRNA-ncRNA and protein–RNA interaction networks from large-scale
634 CLIP-Seq data. *Nucleic Acids Res* **42**, D92–D97 (2014).

635 29. D. W. Huang, B. T. Sherman, R. A. Lempicki, Bioinformatics enrichment tools:
636 paths toward the comprehensive functional analysis of large gene lists. *Nucleic*
637 *Acids Res* **37**, 1–13 (2009).

638 30. D. W. Huang, B. T. Sherman, R. A. Lempicki, Systematic and integrative analysis
639 of large gene lists using DAVID bioinformatics resources. *Nature Protocols* **4**, 44–
640 57 (2009).

641 31. M. Kanehisa, S. Goto, KEGG: Kyoto Encyclopedia of Genes and Genomes.
642 *Nucleic Acids Res* **28**, 27–30 (2000).

643 32. M. Kanehisa, Y. Sato, M. Kawashima, M. Furumichi, M. Tanabe, KEGG as a
644 reference resource for gene and protein annotation. *Nucleic Acids Res* **44**, D457–
645 D462 (2016).

646 33. M. Kanehisa, M. Furumichi, M. Tanabe, Y. Sato, K. Morishima, KEGG: new
647 perspectives on genomes, pathways, diseases and drugs. *Nucleic Acids Res* **45**,
648 D353–D361 (2017).

649 34. H. S. Dengler, G. V. Baracho, S. A. Omori, S. Bruckner, K. C. Arden, D. H.
650 Castrillon, R. A. DePinho, R. C. Rickert, Distinct functions for the transcription
651 factor Foxo1 at various stages of B cell differentiation. *Nature Immunology* **9**,
652 1388–1398 (2008).

653 35. T. Treiber, E. M. Mandel, S. Pott, I. Györy, S. Firner, E. T. Liu, R. Grosschedl,
654 Early B Cell Factor 1 Regulates B Cell Gene Networks by Activation, Repression,
655 and Transcription- Independent Poising of Chromatin. *Immunity* **32**, 714–725
656 (2010).

657 36. H. Maier, R. Ostraat, H. Gao, S. Fields, S. A. Shinton, K. L. Medina, T. Ikawa, C.
658 Murre, H. Singh, R. R. Hardy, J. Hagman, Early B cell factor cooperates with
659 Runx1 and mediates epigenetic changes associated with mb-1 transcription. *Nature*
660 *Immunology* **5**, 1069–1077 (2004).

661 37. R. Song, P. Walentek, N. Sponer, A. Klimke, J. S. Lee, G. Dixon, R. Harland, Y.
662 Wan, P. Lishko, M. Lize, M. Kessel, L. He, miR-34/449 miRNAs are required for
663 motile ciliogenesis by repressing cp110. *Nature* **510**, 115–120 (2014).

664 38. B. Vilagos, M. Hoffmann, A. Souabni, Q. Sun, B. Werner, J. Medvedovic, I. Bilic,
665 M. Minnich, E. Axelsson, M. Jaritz, M. Busslinger, Essential role of EBF1 in the
666 generation and function of distinct mature B cell types. *Journal of Experimental*
667 *Medicine* **209**, 775–792 (2012).

668 39. K. Hutter, T. Rülicke, M. Drach, L. Andersen, A. Villunger, S. Herzog,
669 Differential roles of miR-15a/16-1 and miR-497/195 clusters in immune cell
670 development and homeostasis. *The FEBS Journal* **288**, 1533–1545 (2021).

671 40. M. Coffre, D. Benhamou, D. Rieß, L. Blumenberg, V. Snetkova, M. J. Hines, T.
672 Chakraborty, S. Bajwa, K. Jensen, M. M. W. Chong, L. Getu, G. J. Silverman, R.
673 Blelloch, D. R. Littman, D. Calado, D. Melamed, J. A. Skok, K. Rajewsky, S. B.
674 Koralov, miRNAs Are Essential for the Regulation of the PI3K/AKT/FOXO
675 Pathway and Receptor Editing during B Cell Maturation. *Cell Reports* **17**, 2271–
676 2285 (2016).

677 41. H. Lin, R. Grosschedl, Failure of B-cell differentiation in mice lacking the
678 transcription factor EBF. *Nature* **376**, 263–267 (1995).

679 42. D. W. Harms, R. M. Quadros, D. Seruggia, M. Ohtsuka, G. Takahashi, L.
680 Montoliu, C. B. Gurumurthy, Mouse Genome Editing Using the CRISPR/Cas
681 System. *Current Protocols in Human Genetics* **83**, 15.7.1-15.7.27 (2014).

682 43. C. A. Schneider, W. S. Rasband, K. W. Eliceiri, NIH Image to ImageJ: 25 years of
683 image analysis. *Nat Methods* **9**, 671–675 (2012).

684 44. M. R. Corces, A. E. Trevino, E. G. Hamilton, P. G. Greenside, N. A. Sinnott-
685 Armstrong, S. Vesuna, A. T. Satpathy, A. J. Rubin, K. S. Montine, B. Wu, A.
686 Kathiria, S. W. Cho, M. R. Mumbach, A. C. Carter, M. Kasowski, L. A. Orloff, V.
687 I. Risca, A. Kundaje, P. A. Khavari, T. J. Montine, W. J. Greenleaf, H. Y. Chang,
688 An improved ATAC-seq protocol reduces background and enables interrogation of
689 frozen tissues. *Nat Methods* **14**, 959–962 (2017).

690

691 **Fig. 1. miR-195 promotes HPCs to differentiate into the pro-B cell stage without**
692 **EBF1.**
693 (A) Flow cytometry analysis of control and miR-195-expressing Lin^{-} cells. HPCs from
694 fetal livers of wild-type mice were cultured for 7 days on OP9 with SCF, Flt3-ligand, and
695 IL-7, after infection with control or miR-195 retrovirus. Representative result of control
696 (upper panel) and miR-195 (lower panel) viral infections is shown (n=3). (B) Outline of
697 the *in vitro* culture system of *Ebf1*$^{-/-}$ HPCs. (C) Flow cytometry analysis of control and
698 miR-195-expressing *Ebf1*$^{-/-}$ HPCs. Shown data is representative of n=3. (D) Microarray
699 analysis of miR-195-expressing *Ebf1*$^{-/-}$ HPCs. Log_2 fold-changes in the expression levels
700 of genes related to B (left panel), T (middle-upper panel), NK (middle-lower panel), and
701 myeloid (right panel) cell lineages were classified and are shown as colored columns. The
702 analysis was carried out in duplicates.
703
704 **Fig. 2. miR-195 leads *Ebf1*-deficient HPCs to mature into B cells with bone marrow**
705 **niche assistance.**
706 (A) *In vivo* analysis of B cell development of *Ebf1*$^{-/-}$ HPCs. (B) Flow cytometry analysis
707 of control and miR-195-expressing *Ebf1*$^{-/-}$ HPCs in the bone marrow collected at 7 days
708 after transplantation. (C) Using droplet digital PCR, VJ region fragments were amplified
709 from the genomic DNA of B220^{+} cells in the bone marrow of mice transplanted with
710 control and miR-195-expressing *Ebf1*$^{-/-}$ HPCs. (D) Flow cytometry analysis of control
711 and miR-195-expressing *Ebf1*$^{-/-}$ HPCs in the bone marrow (BM) and spleen (SP), at 10
712 days after transplantation. (E) Flow cytometry analysis of class-switch recombination.
713 Splenocytes of mice transplanted with control and miR-195-expressing *Ebf1*$^{-/-}$ HPCs

714 were cultured for 72 hrs with IgG1 class-switch stimuli, LPS, and IL-4. Each flow
715 cytometric data is representative of *n*=3.
716
717 **Fig. 3. Several B cell populations are disturbed in the miR-195-deficient mice.**
718 Flow cytometry data of B cell lineage populations in miR-195$^{-/-}$ and littermate WT mice.
719 Representative plots (left side) and mean ± S.D. of relative population rates in each
720 littermate WT mice (right side) are shown. (A) Analysis of early B cell populations in the
721 bone marrow. Pre-pro-B (B220^{+} IgM^{-} CD43^{+} CD19^{-}); pro-B (B220^{+} IgM^{-} CD43^{+}
722 CD19^{+}); pre-B (B220^{+} IgM^{-} CD43^{-} CD19^{+}); *n*=5. (B) Analysis of hematopoietic
723 progenitor populations in the bone marrow; *n*=5. (C) Analysis of B cell populations in the
724 spleen. FO B (CD19^{+} IgM^{+} CD21/35$^{low\text{-}middle}$); MZ B (CD19^{+} IgM^{+} CD21/35^{high}); *n*=8.
725 (D) Analysis of B cell populations in the peritoneal cavity: B-1 (B220^{+} CD11b^{+}); B-2
726 (B220^{+} CD11b^{-}); *n*=7. Statistical significance was tested using one-sample *t* test.
727 **p*<0.05; ***p*<0.01. WT, wild-type.
728
729 **Fig. 4. FOXO1 phosphorylation pathways are key targets of miR-195 for promotion**
730 **of B cell development.**
731 (A) Relative expression rate of miR-195 and predicted target genes were compared
732 between control (EMPTY) and miR-195-expressing *Ebf1*$^{-/-}$ HPCs. (B) Relative luciferase
733 inhibitory rates of miR-195 onto predicted target 3′-UTR were analyzed using Dual-
734 Luciferase® reporter assay. (C) Western blot of FOXO1 and phosphorylated FOXO1
735 (pFOXO1) in control and miR-195-expressing *Ebf1*$^{-/-}$ HPCs. Quantification of FOXO1
736 and phospho-FOXO1 band intensities from three independent experiments is shown in
737 the bar graph. Data are presented as mean ± SD. Shown data is representative of *n*=3. (D)

738 Flow cytometry analysis of control and *Foxo1*-expressing *Ebf1*$^{-/-}$ HPCs. Shown data is
739 representative of n=3. Statical significance was tested using one-sample t test. *p<0.05,
740 n=3.
741
742 **Fig. 5. ATAC-seq analysis of *Ebf1*$^{-/-}$ CD19-positive B cells differentiated by miR-195.**
743 (A) Outline of analysis of open chromatin regions in miR-195-expressing *Ebf1*$^{-/-}$ cells.
744 (B) Venn diagram of numbers of genes in which DNA regions of open chromatin peaks
745 were detected by means of peak call analysis. The analyses were examined between
746 CD19-negative (FrA) and -positive (FrB, FrC, and FrD) stages of B cell development
747 (GSE100738; upper red circle); wild-type and *Ebf1*$^{-/-}$ pro-B cells (GSE92434; left-lower
748 blue circle); B220^{+} CD19^{-} cells of control and B220^{+} CD19^{+} positive miR-195-
749 expressing *Ebf1*$^{-/-}$ cells (right-lower green circle). Overlapping regions in the Venn
750 diagram are interpreted as follows: the intersection of WT and Rescue represents
751 canonical EBF1-regulated regions; the overlap between Rescue and miR-195 indicates
752 partial mimicry by miR-195; and regions unique to miR-195 may reflect EBF1-
753 independent chromatin changes. (C and D) Venn diagram of numbers of enriched known
754 motifs detected using HOMER find motif analysis (C) and lists of high p-value motifs,
755 up to rank 10 (D).

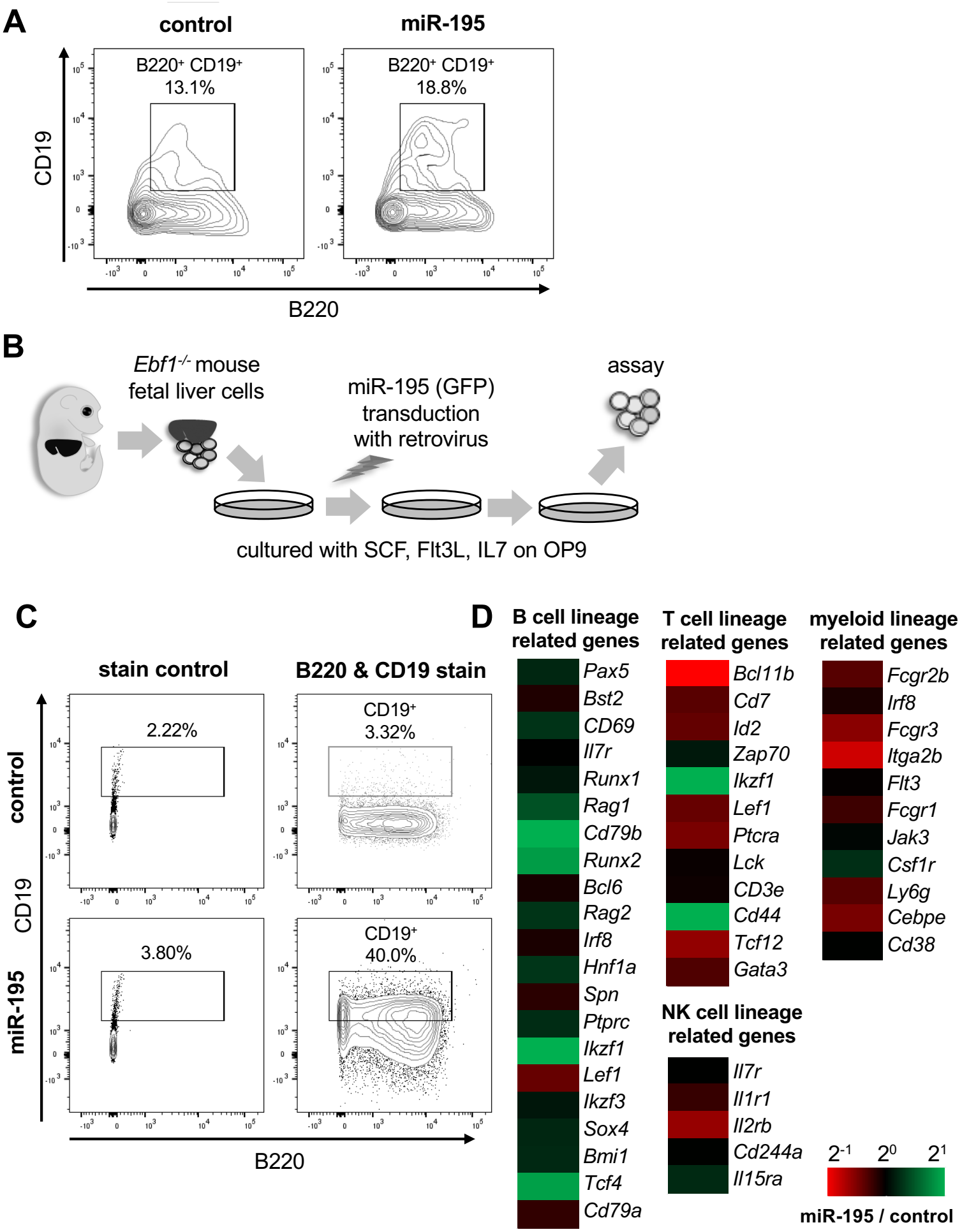
A
control
miR-195
B220+ CD19+
13.1%
B220+ CD19+
18.8%
CD19
B220
B
Ebf1-/- mouse
fetal liver cells
miR-195 (GFP)
transduction
with retrovirus
assay
cultured with SCF, Flt3L, IL7 on OP9
C
stain control
B220 & CD19 stain
control
miR-195
2.22%
CD19+
3.32%
3.80%
CD19+
40.0%
CD19
B220
D
B cell lineage related genes
Pax5
Bst2
CD69
Il7r
Runx1
Rag1
Cd79b
Runx2
Bcl6
Rag2
Irf8
Hnf1a
Spn
Ptprc
Ikzf1
Lef1
Ikzf3
Sox4
Bmi1
Tcf4
Cd79a
T cell lineage related genes
Bcl11b
Cd7
Id2
Zap70
Ikzf1
Lef1
Ptcra
Lck
CD3e
Cd44
Tcf12
Gata3
myeloid lineage related genes
Fcgr2b
Irf8
Fcgr3
Itga2b
Flt3
Fcgr1
Jak3
Csf1r
Ly6g
Cebpe
Cd38
NK cell lineage related genes
Il7r
Il1r1
Il2rb
Cd244a
Il15ra
2-1
20
21
miR-195 / control

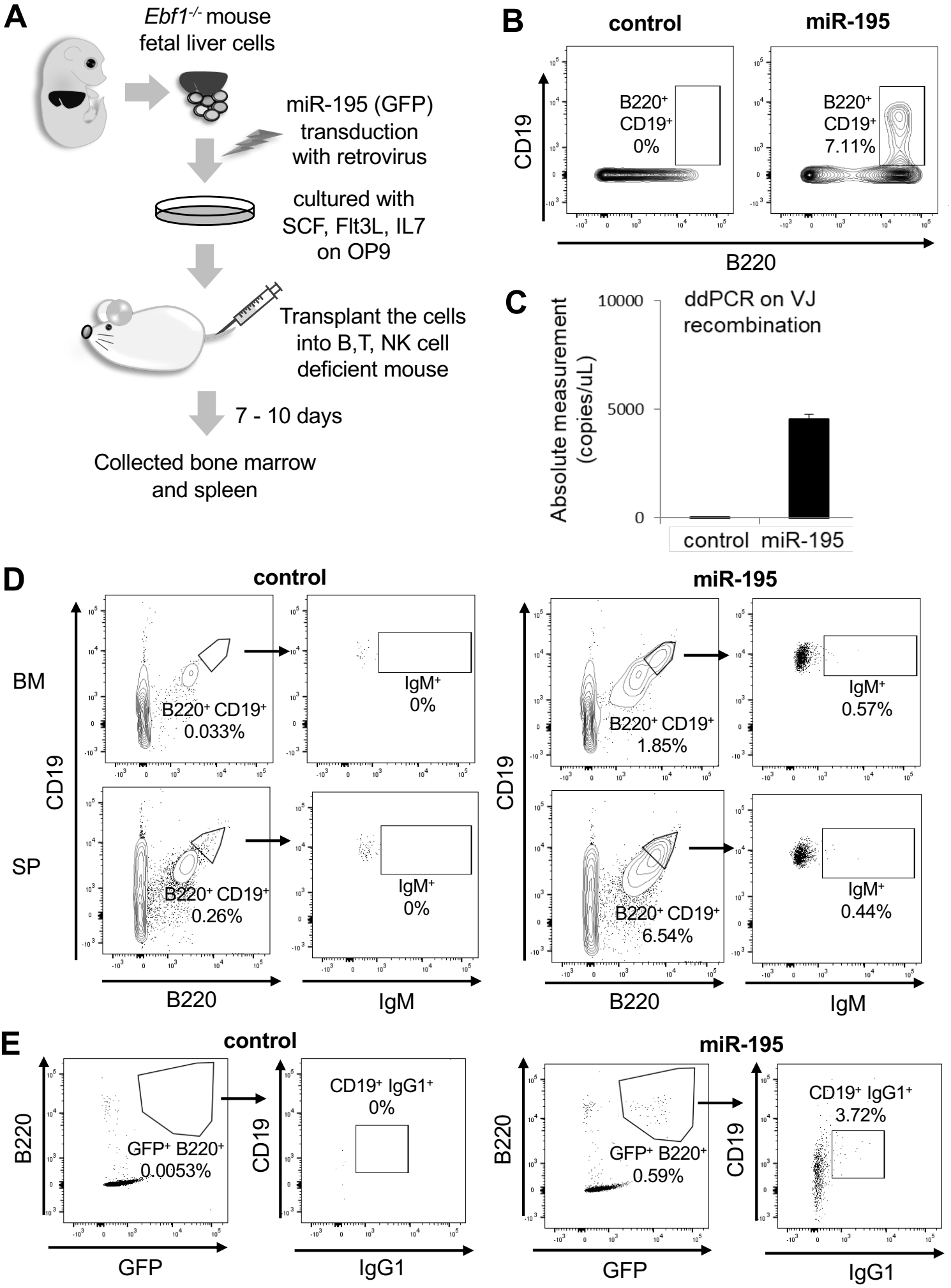
A
Ebf1-/- mouse
fetal liver cells
miR-195 (GFP)
transduction
with retrovirus
cultured with
SCF, Flt3L, IL7
on OP9
Transplant the cells
into B,T, NK cell
deficient mouse
7 - 10 days
Collected bone marrow
and spleen
B
control
miR-195
B220+
CD19+
0%
B220+
CD19+
7.11%
CD19
B220
C
ddPCR on VJ
recombination
Absolute measurement
(copies/uL)
10000
5000
0
control
miR-195
D
control
miR-195
BM
SP
B220+ CD19+
0.033%
IgM+
0%
B220+ CD19+
0.26%
IgM+
0%
B220+ CD19+
1.85%
IgM+
0.57%
B220+ CD19+
6.54%
IgM+
0.44%
CD19
B220
IgM
E
control
miR-195
GFP+ B220+
0.0053%
CD19+ IgG1+
0%
GFP+ B220+
0.59%
CD19+ IgG1+
3.72%
B220
CD19
GFP
IgG1

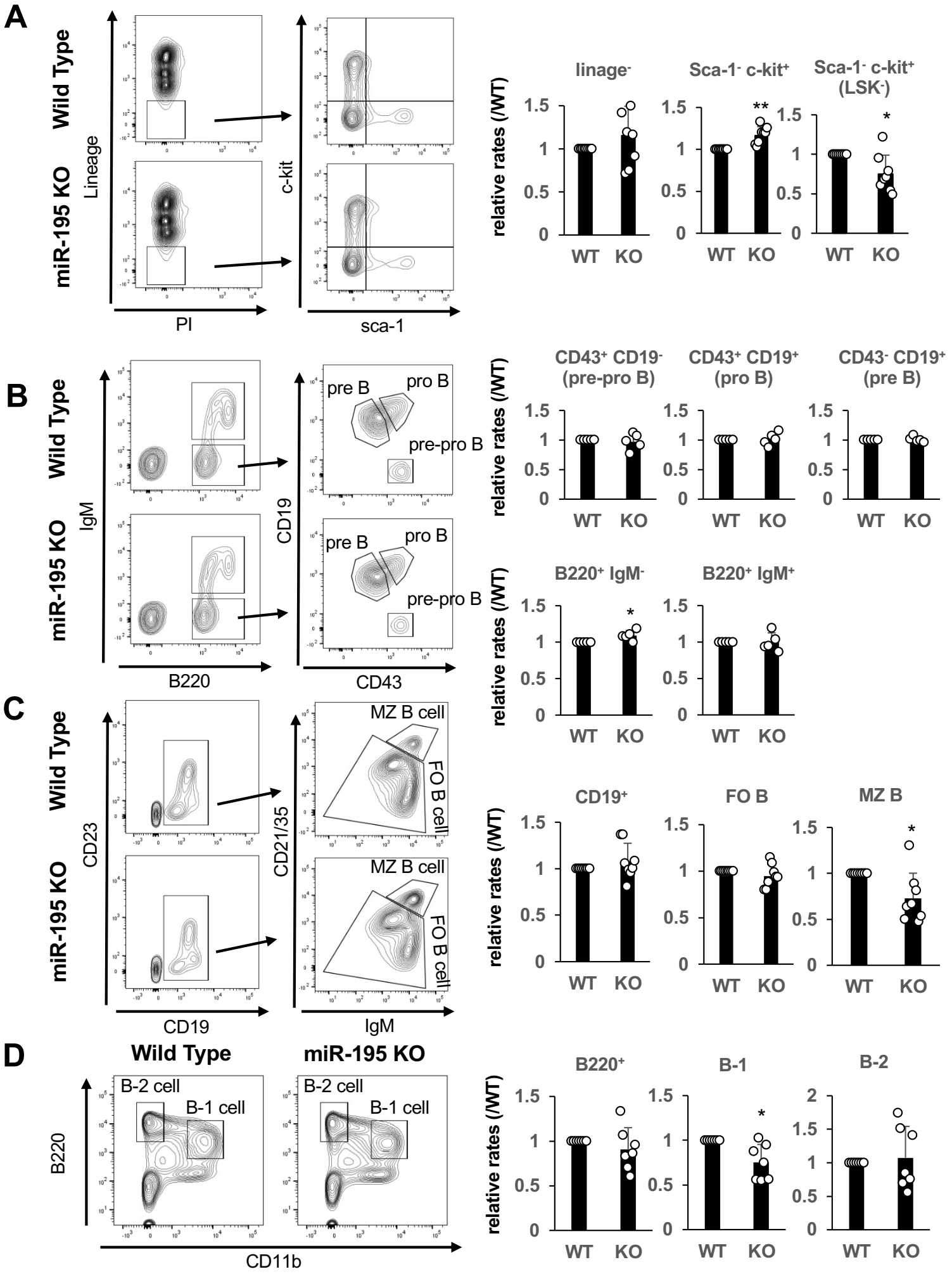
A
Wild Type
miR-195 KO
Lineage
PI
c-kit
sca-1
linage-
Sca-1- c-kit+
Sca-1- c-kit+ (LSK-)
relative rates (/WT)
WT
KO
B
IgM
B220
CD19
CD43
pre B
pro B
pre-pro B
CD43+ CD19- (pre-pro B)
CD43+ CD19+ (pro B)
CD43- CD19+ (pre B)
B220+ IgM-
B220+ IgM+
C
CD23
CD19
CD21/35
IgM
MZ B cell
FO B cell
CD19+
FO B
MZ B
D
Wild Type
miR-195 KO
B220
CD11b
B-2 cell
B-1 cell
B220+
B-1
B-2

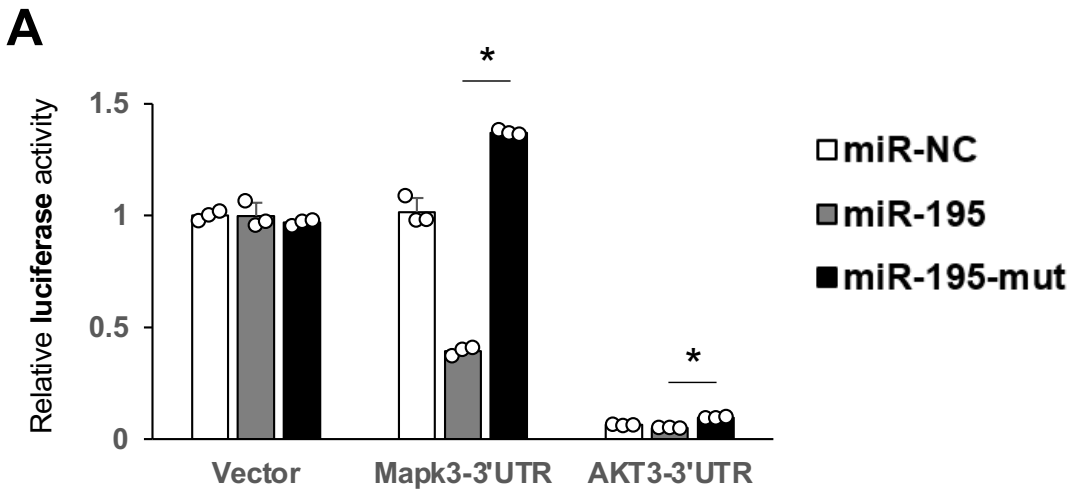
A
Relative luciferase activity
1.5
1
0.5
0
*
*
miR-NC
miR-195
miR-195-mut
Vector
Mapk3-3'UTR
AKT3-3'UTR

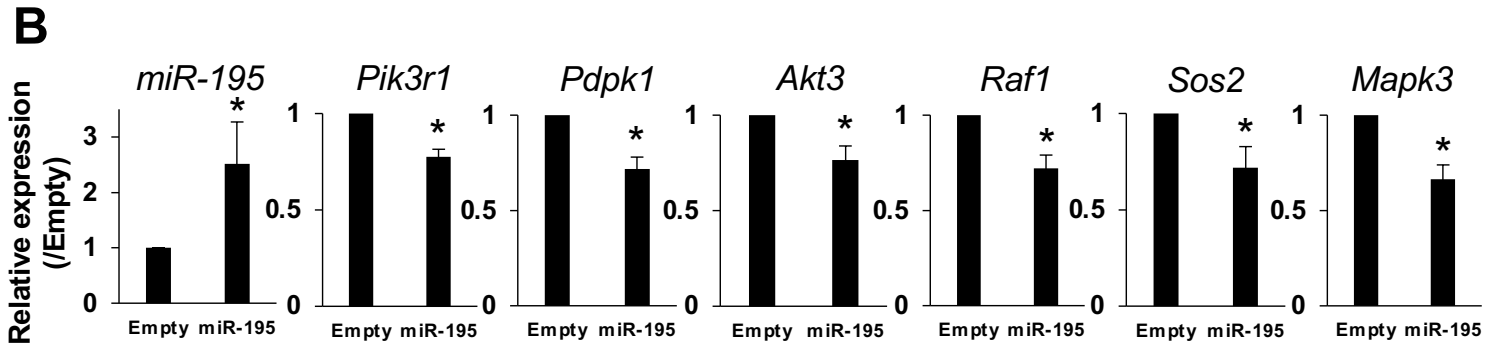
B
Relative expression (/Empty)
miR-195
Pik3r1
Pdpk1
Akt3
Raf1
Sos2
Mapk3
Empty
miR-195

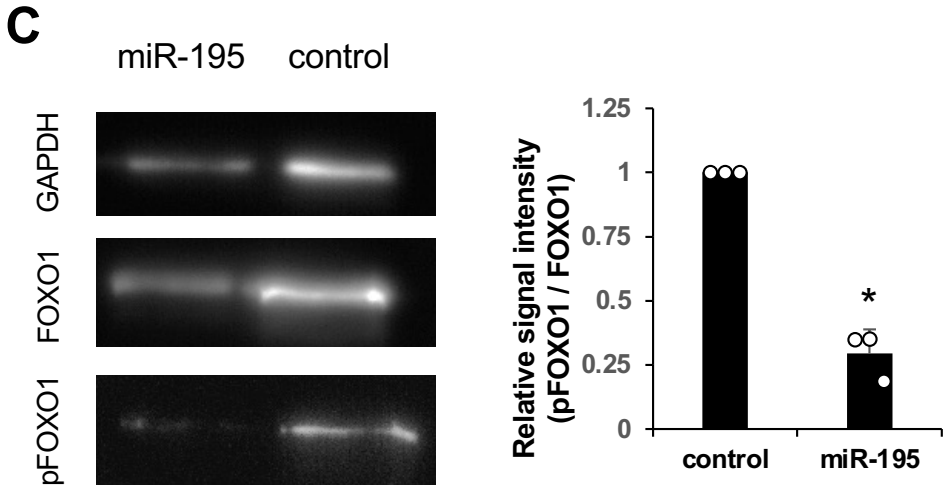
C
miR-195
control
GAPDH
FOXO1
pFOXO1
Relative signal intensity (pFOXO1 / FOXO1)
1.25
1
0.75
0.5
0.25
0
control
miR-195

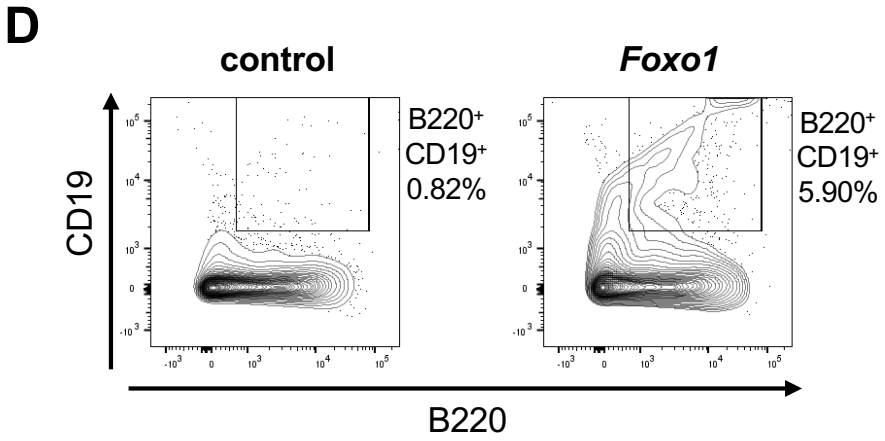
D
control
Foxo1
CD19
B220
B220+
CD19+
0.82%
B220+
CD19+
5.90%

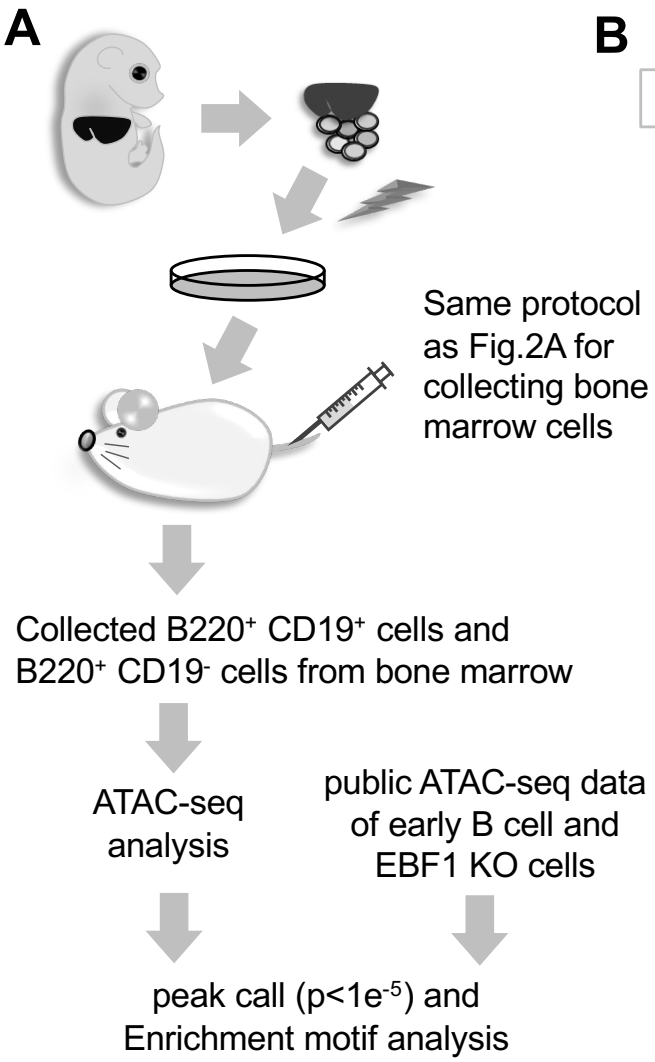

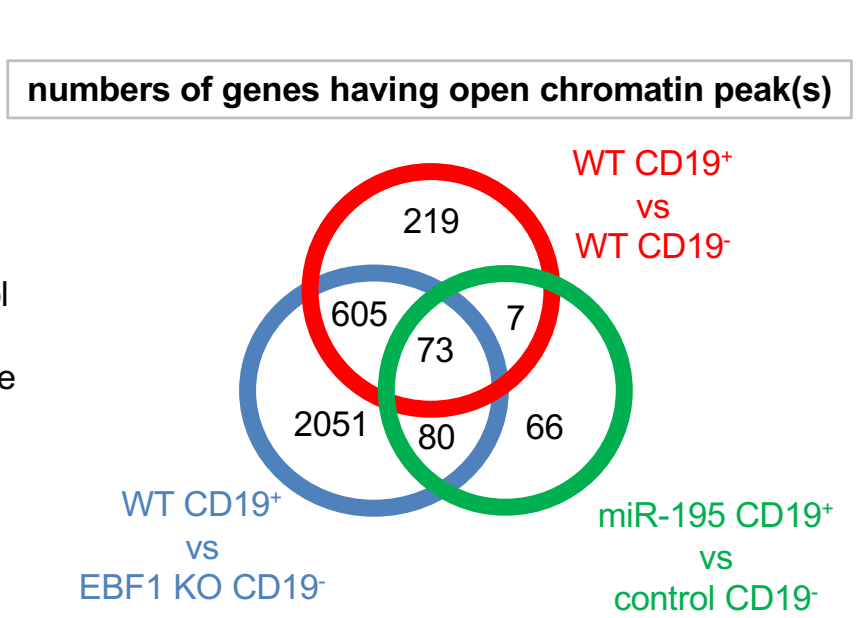

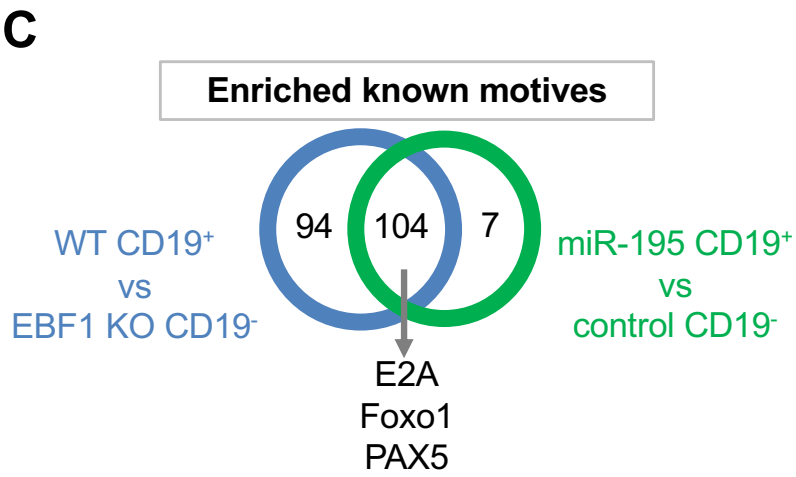

D

WT CD19+ vs EBF1 KO CD19-

Rank	Motif	Name	P-value
1		EBF2(EBF)/BrownAdipose-EBF2-ChIP-Seq(GSE97114)/Homer	1e-111
2		EBF(EBF)/proBcell-EBF-ChIP-Seq(GSE21978)/Homer	1e-104
3		Etv2(ETS)/ES-ER71-ChIP-Seq(GSE59402)/Homer	1e-810
4		ERG(ETS)/VCaP-ERG-ChIP-Seq(GSE14097)/Homer	1e-796
5		ETS1(ETS)/Jurkat-ETS1-ChIP-Seq(GSE17954)/Homer	1e-760
6		Fli1(ETS)/CD8-FLI-ChIP-Seq(GSE20898)/Homer	1e-706
7		ETV1(ETS)/GIST48-ETV1-ChIP-Seq(GSE22441)/Homer	1e-702
8		Ets1-distal(ETS)/CD4+-PolII-ChIP-Seq(Barski_et_al.)/Homer	1e-663
9		EWS:ERG-fusion(ETS)/CADO_ES1-EWS:ERG-ChIP-Seq(SRA014231)/Homer	1e-661
10		GABPA(ETS)/Jurkat-GABPa-ChIP-Seq(GSE17954)/Homer	1e-618

miR-195 CD19+ vs control CD19-

Rank	Motif	Name	P-value
1		Etv2(ETS)/ES-ER71-ChIP-Seq(GSE59402)/Homer	1e-55
2		ERG(ETS)/VCaP-ERG-ChIP-Seq(GSE14097)/Homer	1e-54
3		Fli1(ETS)/CD8-FLI-ChIP-Seq(GSE20898)/Homer	1e-54
4		ETV1(ETS)/GIST48-ETV1-ChIP-Seq(GSE22441)/Homer	1e-49
5		ETS1(ETS)/Jurkat-ETS1-ChIP-Seq(GSE17954)/Homer	1e-49
6		PAX5(Paired,Homeobox)/GM12878-PAX5-ChIP-Seq(GSE32465)/Homer	1e-45
7		Ets1-distal(ETS)/CD4+-PolII-ChIP-Seq(Barski_et_al.)/Homer	1e-40
8		EWS:ERG-fusion(ETS)/CADO_ES1-EWS:ERG-ChIP-Seq(SRA014231)/Homer	1e-40
9		ETV4(ETS)/HepG2-ETV4-ChIP-Seq(ENCODE)/Homer	1e-38
10		PU.1(ETS)/ThioMac-PU.1-ChIP-Seq(GSE21512)/Homer	1e-34